VETP - SHORT COURSE ON NEW TECHNIQUES FOR ASSESSING AND QUANTIFYING VESSEL STABILITY AND SEAKEEPING QUALITIES

MARINTEK, Trondheim 8 - 11 March 1993

Participants:

Company	Name:
Abeking & Rasmussen, Germany	Erwin Karabinski, Dipl.Ing.
Brodosplit, Jugoslavia	Damir Bezinovic, Naval Architect
Danyard A/S, Denmark	Christian Schack, Naval Architect
Gusto Engineering bv, Holland	Carlo van dee Stoep, Senior Eng. Spec.
Insean, Italy	Dr. R. Penna
Karlskronavarvet AB, Sweden	Jan Bergholtz, Naval Architect Mats Olsson, Naval Architect
Kværner Masa-Yards, Finland	Ismi Lindstrøm
Ministry of Defence Royal Netherlands Navy, The Netherlands	J.L. Perluka, R. Brouwer
Netherlands Coast Guard, The Netherlands	A. Schaap, Ing./Naval Architect
Norwegian Marine Directorate	Dag Liseth, Div. Eng.
Sedco-Forex, France	Georges Barreau, Naval engineer
SSPA Maritime Consulting AB, Sweden	Jan Lundgren
STN Systemtechnic Nord, Germany	Frank Meyer, Dipl. Ing.

POSITION CONTROL - FROM ANCHORING TO DP SYSTEMS

by

Dr J.E.W. Wichers
Maritime Research Institute Netherlands

INTRODUCTION

In the last decade the design of offshore mooring systems and the offloading techniques have changed. The changes in the developments have been made possible by a few important achievements as for instance:
- the increased reliability of flexible risers;
- better understanding of the low frequency motion behaviour of moored ships in waves, wind and current;
- prototype experience with the increasing number of moored Floating (Production) Storage Offloading (F(P)SO) systems;
- application of dynamic positioning (DP) on large offloading tankers.

Modern designs of F(P)SOs and Offshore Loading Systems (OLS) are a reduction of the large variety in the past. In the past typical systems designed and applied were the compliant articulated systems. The following concepts apply to the majority of the present offshore designs:
- For permanent mooring systems: internal or external turrets, in many cases provided with composite lines.
- For semi-permanent mooring systems: disconnectable underkeel buoy or riser turrets and DP systems.
- For offloading: tandem mooring and DP.

For the design of the systems in the pre-design stage semi-theoretical empirical mathematical simulation models can be applied, while for the verification of the design model experiments are indispensable. In the design process the physical phenomena which control the motions of a moored or DP tanker must be understood. The physical phenomena are the exciting loads, the reaction forces and the motion control system (mooring system or DP control). A review will be given of the basic approaches to assess the motion control of a permanently moored and a DP controlled tanker exposed to wind, waves and current.

THE TANKER MOTIONS

A tanker kept in position in irregular waves, wind and current will be exposed to wave frequency loads in the six degrees of freedom (DOF) and mean loads in combination with slowly varying loads in the three DOFs in the horizontal plane.

The wave frequency loads are caused by the well-known first order wave forces. The mean loads are due to mean wave drift force,

current and wind loads. The slowly oscillating loads are caused by the second order slowly oscillating wave drift forces and loads as induced by the low frequency components of the wind speed spectrum. In some cases low frequency excitation can even occur due to macro vortices in a turbulent current or due to shedding from the vessel itself.

The result is that the vessel will perform wave frequency motions and at the same time is subjected to a mean displacement and low frequency motions. The wave frequency motions introduce the wave frequency dynamics in the mooring legs of a mooring system. For DP systems the wave frequency motions can affect the effectivity of the thrusters. The most important part of the power needed for station keeping of a tanker is caused by the mean displacement and the low frequency motions. The control system of a DP system has to react to these motions, while the force level in a mooring system will be dominated by these motions.

In order to describe the low frequency motions the wave drift forces, the wind and current loads and the low frequency hydrodynamic reaction forces have to be known. Each of the mentioned components will be briefly described in the next sections.

WIND, CURRENT AND WAVE DRIFT FORCES ON A TANKER

Current and wind loads

For a tanker-based FPSO the current loads can be derived from the updated current coefficients as given by OCIMF. The coefficients in longitudinal, transverse and yaw direction will be given not only for the fully loaded draft as function of the ratio draft/water depth but also for the ballasted condition (even keel) of tankers with cylindrical and conventional bow.

Wind load data for a tanker with standard superstructure and without process equipment can be found with the OCIMF data. To account for the process equipment and possible interaction with the superstructure computer programs based on wind tunnel tests are available or wind tunnel tests have to be carried out.

Wind spectra

Because of the importance of the low frequency excitation on moored structures wind spectra can be applied to the tanker. The spectral density in the low frequency part of the wind spectra can be considerable. For various formulations of wind spectra the spectra based on an hourly mean wind speed of 30.9 m/s (10 m elevation) is given in Fig. 1. In [1] the results are given of the effect of the application of wind spectra and a 1-minute gust on a moored 200 kDWT tanker in co-linearly directed irregular waves and wind.

The results show that due to the 1-hour mean wind speed the mean displacement is small but that the oscillating wind force causes

a most probable surge motion which generally is lower than the values found for the steady 1-minute gust.

Wave-current interaction on wave drift forces

The wave drift forces contribute generally for a dominant part to the total low frequency excitation on a moored or DP controlled tanker. In order to determine the mean and slowly oscillating wave drift force it is common practice to compute the quadratic transfer function (QTF). By means of spectral or time domain techniques the mean and the oscillating wave drift force can be determined. The computations are based on 3-D potential theory and are valid for the zero-speed condition, see for instance [2].

The QTF of the wave drift force on a tanker may increase considerably when moored in a current field. In the zero-current condition the speed dependency of the wave drift force due to the slowly oscillating moored tanker will be present also. This speed dependency of the wave drift force can be distinguished by the QTF of the wave drift damping. In case the tanker is moored in waves combined with current the wave drift force can be described by the current speed dependent QTF. The slowly oscillating motions of the vessel in the current field are governed by the current speed associated QTF and the current speed associated QTF of the wave drift damping. For head waves the computation procedures are given in [3]. As an example the QTF of the wave drift force with and without current and the wave drift damping for an LNG carrier is given in Fig. 2.

Besides the QTF in head waves and head current, also the wave drift forces for waves combined with arbitrarily directed current are necessary. The general computation procedure is under development, see [4]. An example of the QTF for another direction of wave and current is shown in Fig. 3.

LOW FREQUENCY HYDRODYNAMIC REACTION FORCES

In the aforementioned section the mean and low frequency excitation forces are briefly explained. Due to the excitation the moored or DP controlled vessel will perform low frequency motions in the horizontal plane. Besides the mooring and DP system also hydrodynamic forces will react to the slowly oscillating displacements, velocities and accelerations. The low frequency hydrodynamic reaction forces can be split in the acceleration and velocity dependent terms. The acceleration terms consist of the low frequency added mass and can be computed with 3-D potential theory. The low frequency velocity dependent terms, however, consist of the viscous resistance. These terms cannot be computed accurately and have to be derived from model tests.

For the derivation of the low frequency hydrodynamic reaction forces and moment distinction has to be made between still water and current. Compared to the still water resistance it is obvious that the resistance forces/moment may strongly be influenced by the presence of the current (lift and drag forces).

In the following the description of the low frequency hydrodynamic reaction forces in terms of the equations of motion will be elucidated.

Still water

For the equations of motion the following formulations are assumed, see [3]:

$$(M+a_{11})\ddot{x}_1 = (M+a_{22})\dot{x}_2\dot{x}_6 + a_{26}\dot{x}_6^2 + X_{1SW}$$

$$(M+a_{22})\ddot{x}_2 + a_{26}\ddot{x}_6 = -(M+a_{11})\dot{x}_1\dot{x}_6 + X_{2SW}$$

$$(I+a_{66})\ddot{x}_6 + a_{62}\ddot{x}_2 = -(a_{22}-a_{11})\dot{x}_1\dot{x}_2 - a_{62}\dot{x}_1\dot{x}_6 + X_{6SW}$$

in which:

X_{1SW}, X_{2SW}, X_{6SW} = low frequency viscous fluid resistance forces/moment components
a_{11}, a_{22}, a_{66}, a_{26}, a_{62} = low frequency added mass coefficients
x_1, x_2, x_6 = surge, sway and yaw motion
M, I = inertia properties of the vessel.

In order to determine the low frequency viscous resistance force/moment components in still water caused by sway and yaw modes of motion, planar motion mechanism tests may be carried out. For the surge mode of motion extinction tests in still water can be carried out. The resistance coefficients as derived from the extinction tests in surge direction are given in Fig. 4. The resistance coefficients in the sway and yaw direction are given in Fig. 5. For the sway direction the damping coefficient B_{22} and B_{62} were obtained as follows:

$$X_{22} = -\tfrac{1}{2}\rho\, T\, B_{22} \int_{AP}^{FP} \dot{x}_2|\dot{x}_2|\,dl = -\tfrac{1}{2}\rho\, T\, B_{22}(FP-AP)\dot{x}_2|\dot{x}_2|$$

$$X_{62} = -\tfrac{1}{2}\rho\, T\, B_{62} \int_{AP}^{FP} \dot{x}_2|\dot{x}_2|\,l\,dl = -\tfrac{1}{2}\rho\, T\, B_{62}(FP^2-AP^2)\dot{x}_2|\dot{x}_2|$$

while in yaw direction the coefficients B_{26} and B_{66} can be determined from:

$$X_{26} = -\tfrac{1}{2}\rho\, T\, B_{26} \int_{AP}^{FP} \dot{x}_6 l|\dot{x}_6 l|\,dl = -\tfrac{1}{6}\rho\, T\, B_{26}(FP^3+AP^3)\dot{x}_6|\dot{x}_6|$$

$$X_{66} = -\tfrac{1}{2}\rho\, T\, B_{66} \int_{AP}^{FP} \dot{x}_6 l|\dot{x}_6 l|\,l\,dl = -\tfrac{1}{8}\rho\, T\, B_{66}(FP^4+AP^4)\dot{x}_6|\dot{x}_6|$$

in which:

X_{22}, X_{62}, X_{26}, X_{66} = measured forces/moment, in-quadrature with the applied displacements
AP = ordinate of aft perpendicular
FP = ordinate of fore perpendicular.

Knowing the resistance coefficients B_{22}, B_{26}, B_{62} and B_{66} the coupled sway and yaw low frequency resistance forces/moment can be described assuming a strip type distribution of the transverse coefficients over the length of the vessel. Decoupled in surge direction the resistance formulations are as follows:

$$X_{1SW} = -B_{11}\dot{x}_1$$

$$X_{2SW} = -\tfrac{1}{2}\rho\, T \int_{AP}^{FP} C(l)(\dot{x}_2+\dot{x}_6 l)|\dot{x}_2+\dot{x}_6 l|\,dl$$

$$X_{6SW} = -\tfrac{1}{2}\rho\, T \int_{AP}^{FP} C(l)(\dot{x}_2+\dot{x}_6 l)|\dot{x}_2+\dot{x}_6 l|\,l\,dl$$

In current

For the equations of motion the following formulations are assumed, see [3]:

$$(M+a_{11})\ddot{x}_1 = (M+a_{22})\dot{x}_2\dot{x}_6 + X_{1stat} + X_{1dyn}$$

$$(M+a_{22})\ddot{x}_2 + a_{26}\ddot{x}_6 = -(M+a_{11})\dot{x}_1\dot{x}_6 + X_{2stat} + X_{2dyn}$$

$$(I_6+a_{66})\ddot{x}_6 + a_{62}\ddot{x}_2 = X_{6stat} + X_{6dyn}$$

in which:

$$X_{1stat} = \tfrac{1}{2}\rho\, L\, T\, C_{1c}(\psi_{cr})V_{cr}^2$$
$$X_{2stat} = \tfrac{1}{2}\rho\, L\, T\, C_{2c}(\psi_{cr})V_{cr}^2$$
$$X_{6stat} = \tfrac{1}{2}\rho\, L^2 T\, C_{6c}(\psi_{cr})V_{cr}^2$$

being the quasi-steady current forces/moment components, where:

$V_{cr} = (u_r^2 + v_r^2)^{\frac{1}{2}}$ = relative current velocity

$\psi_{cr} = \arctan(-v_r/-u_r)$ = relative current angle of incidence

and the dynamic current load contribution is assumed to be:

$$X_{1dyn} = -(a_{22}-a_{11})V_c \sin(\psi_c-x_6)\dot{x}_6 + X_{1D}$$

$$X_{2dyn} = -(a_{22}-a_{11})V_c \cos(\psi_c-x_6)\dot{x}_6 + X_{2D}$$

$$X_{6dyn} = \underbrace{\qquad\qquad}_{\text{potential part}} + \underbrace{X_{6D}}_{\text{viscous part}}$$

To determine the dynamic current contribution as acting on a tanker, yaw and sway oscillation tests may be carried out in current. A typical result of a model test to determine the dynamic current contribution in surge, sway and yaw direction due to the motion in yaw direction in 2 knots current is given in Fig. 6. By means of the dynamic current load contributions as function of current speed, oscillating velocities and current angles a non-dimensional database can be established.

By means of the above given descriptions the low frequency hydrodynamic reaction forces can be implemented in the equations of motion.

PERMANENT MOORING SYSTEM

Introduction

An example of a permanent mooring system can be a turret-chain system. The turret is a turntable connected to the bow or to the keel of a tanker. To keep the tanker in position radially spaced mooring lines are attached to the top of the turntable. The number of mooring legs can range from 6 up to 12 or more. A sketch of such a system is given in Fig. 7. In the turntable swivels are mounted for transfer of the oil. The oil is transported through flexible risers running from the turntable to subsea wells or pipeline end manifolds.

In order to design the mooring system pre-studies and model tests have to be carried out. From the results of the pre-study and the model tests the size and pattern of the mooring legs (chains or chain-wire combinations), the position of the turntable (stability) and the strength (survival and fatigue loads) have to be obtained. Besides these aspects also attention has to be paid to the layout of the flow/control lines.

Further attention has to be paid to the statistics of the input and output. The input concerns the statistics of the wave, wind and current climate like the determination of their proper probabilistic joint occurrence. The results of the computer simulations and the model tests are the output. The statistical evaluation of the results like confidence intervals of the most probable maximum, joint probability of low and wave frequency quantities and extreme effects such as slamming and green water have to be carefully considered. A review of the probabilistics

for the input data and the statistics of the output is given in [5].

As an introduction a simplified exercise will be carried out to assess the low frequency motions of a moored 200 kDWT loaded tanker. This exercise is followed by a brief description of the method of the complete analysis on a turret moored tanker in irregular head waves.

Simplified method to assess the low frequency tanker motions

For the simplified exercise use is made of a fully loaded 200 kDWT tanker co-linearly moored in irregular waves and current. The mooring system consists of a linear spring above water in surge direction of the tanker. The tanker is moored in 82.5 m water depth. The body plan of the tanker, the main particulars and input data like QTF of the wave drift forces and the wave drift damping are given in [3]. The exercise concerns the effect of the current and the stiffness of the mooring on the low frequency motions. Therefore computations are carried out with 2 knots current and without current and with two stiffnesses of the mooring system viz. 6.8 tf/m and 60 tf/m.

Because of the linearity of the equation of motion of the low frequency motions in surge direction the computations can be carried out in the frequency domain. The computation procedure is given below. In the frequency domain the variance of the low frequency surge motion will be, see [3]:

$$\sigma^2_{x_1} = \frac{\pi}{2\ b\ c_{11}} \cdot S_F(\mu_e)$$

and the most probable maximum displacement according to Longuet-Higgins gives:

$$x_{1max} = \bar{x}_1 + \sqrt{2} \cdot \sigma_{x_1} \sqrt{\ln N}$$

in which:

b = total displacement

c_{11} = spring constant

N = number of oscillations = $\frac{\text{duration of time}}{\text{natural period of system}}$

$\bar{x}_1 = \bar{X}_{1t}/c_{11}$ = mean displacement of the tanker

$\bar{X}_{1t}$ = total mean force.

The mean drift force in irregular waves becomes:

$$\bar{F} = 2 \int_0^\infty S_\zeta(\omega)\ T(\omega,\omega)\ d\omega$$

The mean wave drift damping coefficient will be:

$$\bar{B}_1 = 2 \int_0^\infty S_\zeta(\omega) \frac{B_1(\omega)}{\zeta_a^2} d\omega$$

while the spectral density of the force becomes:

$$S_F(\mu) = 8 \int_0^\infty S_\zeta(\omega+\mu)\ S_\zeta(\omega)\ T^2(\omega+\mu,\omega)\ d\omega$$

where:

$S_\zeta(\omega)$ = spectral density of the wave elevation

$T(\omega,\omega)$ = continuous equivalent of the discrete $T_{ii} = (\omega_i,\omega_i)$

$B_1(\omega)/\zeta_a^2$ = quadratic transfer function of the wave drift damping

$T(\omega+\mu,\omega)$ = continuous equivalent of the discrete quadratic transfer function for the amplitude of the drift force $T_{ij} = T(\omega_i,\omega_j)$ with $\omega_i \geq \omega_j$

μ = difference frequency ≥ 0

$S_F(\mu)$ = spectral density of the drift force

$\bar{F}$ = mean value of the drift force

$\bar{B}_1$ = mean wave drift damping coefficient.

For the wave spectrum a Pierson-Moskowitz type spectrum with a significant wave height H_s = 10 m and a mean period T_1 = 12 s was chosen. The computed spectral densities are shown in Fig. 8.

The low frequency viscous surge damping coefficient without current is derived from Fig. 4, while for the current damping coefficient the following formula is used:

$$b_{11c} = 2F_c/V_c$$

in which F_c is the mean current force in longitudinal direction and V_c is the current velocity.

The results of the computations are given in Table 1 on the next page.

For the simplified approach the computation procedure has been shown to calculate the motions of a linearly moored tanker. In an irregular sea combined with current both the mean wave drift force and the slowly oscillating part of the wave drift force will increase considerably due to the current effect. As a result the motions are larger in a current field than in the non-current condition.

Comparing the results in the non-current condition with different springs it can be noticed that the spectral density of the wave drift force considerably decreases with a stiffer mooring system. The relation between the spectral density and the natural period of the system is shown in Fig. 8.

Because of the increased stiffness and the decreased spectral density the motions will decrease. The mooring forces, however, will be increased approximately by a factor 2 compared with the softer mooring system.

Table 1

		Without current	With current (2 kn)	Without current
		c_{11} = 6.8 tf/m	c_{11} = 6.8 tf/m	c_{11} = 60 tf/m
$M+a_{11}$	$tf.s^2/m$	26,145.4	26,145.4	26,145.4
μ_e	rad/s	0.0161	0.0161	0.0479
T_e	s	390	390	131
t	s	9000	9000	9000
N	-	23	23	68.7
$\overline{F}$	tf	-85.6	-103.8	-85.6
F_c		-	-10.4	-
$\overline{B}_1$	tf/m/s	29.0	25.7	29.0
B_{11}	tf/m/s	16.0	-	23.0
b_{11c}	tf/m/s	-	20.2	-
b	tf/m/s	45.0	45.9	52.0
$S_F(\mu_e)$	$tf^2.s$	27,700.0	43,000.0	15,000.0
σ_x	m	11.92	14.71	2.75
$\overline{x}_1$	m	-12.59	-16.79	-1.43
x_{1max}	m	-42.45	-53.63	-9.43
X_{1max}	tf	288.7	364.7	565.8

Complete simulations

For the complete simulation a turret-chain system exposed to irregular waves is considered. The configuration of the system is shown in Fig. 7.

In a static sense the reaction force on the tanker moored by a chain-turret system represents the load displacement curve, being the restoring force. In reality, due to the low and wave frequency motions of the turret, the chains are moving through the

fluid. The chain forces will not only be influenced by the static load curve, but also by the forces caused by the velocity and acceleration dependent hydrodynamic loading (the Morison equation) and the chain inertia forces along the chain length. The result is that the static load curve can strongly deviate from the momentaneous mooring forces. In the time domain, due to the low and high frequency motions of the turret, the "static load" will be stiffened or weakened. Due to the "stiffening" and the "weakening" of the static load curve the low frequency motions of the tanker can be strongly influenced. In fact, the time average over the content of the hysteresis of the horizontal dynamic mooring force versus displacement is called the "low frequency chain damping".

To take into account the time dependent "low frequency chain damping", the complete integrated system of chain-turret moored tanker has to be simulated in the time-domain with the correct coupling between the high and low frequency motions.

The mooring system is modelled by means of the lumped mass method, where each of the mooring legs is represented by a large number of discrete elements. On each nodal point the segment tension, weight, fluid forces and bottom reaction forces will be taken into account. Because of the direct time-domain simulation method the dynamic behaviour of the mooring chains must be modelled correctly, resulting in small time steps in the integration method (0.05 s).

The convolution integrals of the first and second order wave forces are taken at the momentaneous position of the tanker in the irregular wave field resulting in the exact wave loading on the tanker at each time step. Further, the hydrodynamic reaction forces were obtained by the Cummins impulse response functions, while the viscous surge damping of the tanker was taken from Fig. 4.

The computations were applied to a 200 kDWT loaded tanker in 82.5 m water depth exposed to a PM spectrum with H_s = 9.8 m and T_1 = 13.0 s. The layout of the mooring pattern consists of 6 chains, each 700 m long. The pre-tension amounts to 40.83 tf and the chain diameter is 5.5 inches.

The results of the model tests and the computations using the same wave train are given in a sample time history in Fig. 9. From the results it can be concluded that a good comparison is achieved. For more information reference is made to [6] and [7].

DYNAMIC POSITIONING

Introduction

Nowadays DP tankers may be used as an alternative for hawser type mooring, for tandem mooring and for offshore buoy loading systems. A well-known buoy loading system is the UKOLS system at the Statfjord field; careful experiments have been carried out for DP

offloading in tandem configuration (in full scale as well as in model tests). It can be observed that there is a growing tendency at new field developments to use dynamically positioned systems instead of bow hawser moorings.

The conventional method of DP implies position as well as heading control of the ship, an approach which requires substantial side thrust capacity at the stern of the ship. The consequence is the application of a twin screw arrangement with high performance rudders. Also, the fitting of tunnel or azimuthing thrusters aft is costly, even on a single screw tanker, due to the presence of engine room and shaft arrangement. The application of bow loading with weather following DP will improve the workability and reliability of the DP offloading concept, and since there is no need of side thrust capacity at the stern, reduced capital expenditure for the DP equipment on the export tanker follows.

The hydrodynamic investigations for a DP system are carried out in two phases:

- A pre-study in which computer calculations and simulations are carried out. Herein physical trends can be investigated and a concept exploration can be made. Although DP simulations are instructive, the same holds true as for mooring simulations: the results are not to be used for the final design data.
- For reliable design data, relating the available power and thruster capabilities to the positioning accuracy and limits of "workability", it is possible to carry out closed loop DP tests.

DP simulations

Computer programs for DP simulations basically carry out a control loop in which the ship position is given by the hydrodynamic mathematical model which is also used for mooring simulations, see [3]. The position difference with the required set-point for dynamic positioning, and the ship horizontal velocities are inputted to the control algorithm for thruster action, see [8].

For the control algorithm the effective forces generated by the thrusters, propellers and rudders have to be known. The effective forces can differ widely from the bollard pull values. This is caused by both thruster-thruster, thruster-hull, propeller-hull, rudder-propeller-hull interaction as well as interaction with the current. The hull and current types of interaction are to be attributed to the changes in the pressure distribution on the hull induced by the working propellers, rudders and thrusters as compared to the pressure distribution due to current only.

Fig. 10 gives an example of typical pressure distribution changes for a bow thruster operating whilst the vessel is subjected to a certain head current. The low pressure region downstream of the jet exit side is the dominant factor and integrates to an appreciable side force opposite to the thrust T, thus reducing the effective side force of the thruster.

Fig. 11 shows the results of thruster-thruster interaction under a flat plate for azimuthing thrusters. In the graphs the interaction as function of the distance between two thrusters and as function of azimuth angle of the forward thruster is shown.

By means of computations, see [9], and/or a set of separate model tests the effectivity values of the thrusters, rudders and propellers can be determined. Using the proper effectivity values in the control algorithm the performance of the ship will be improved.

Usually the simulation programs are limited to low frequency motions only, which is sufficient in most applications. However, when a ship is equipped with bow tunnels, and its draft (or sea state) is such that frequent bow tunnel emergence occurs, significant degradation of thruster effectivity will be the result as is shown in Fig. 12. Try-out of computer simulations in an irregular sea with this type of degradation is carried out. The results are shown in Fig. 13.

On basis of computer simulations it is possible to select an optimum concept for the DP in terms of:
- thruster arrangement and type;
- location and power of thrust units;
- mode of DP: full position and heading control or weather DP;
- safety and redundancy evaluation.

By means of the computations for different DP concepts the limiting sea state can be determined in which -with the selected thruster configuration- the tanker can stay sufficiently accurate in position.

Physically, the limit for DP is the result of a combination of effects as is shown in Fig. 14. In the figure relating positioning accuracy and sea state, four different regions can be discerned. In the first and second region the positioning is accurate. In the third region the environmental loads on the tanker are so high that the thrust requirements exceed the available capacity for relatively long periods of time. In this situation the positioning accuracy deteriorates although the positioning is still stable and feasible. In the fourth region, the positioning error increases rapidly. The maximum excursions are very large and the risk exists that the position gets lost, either due a high wave group or due to the impossibility to keep station.

Furthermore, specific events, such as the ship response to reference failure, sudden wind changes and thruster failure or application of wave feed forward can be investigated. By means of this information a model test program can be optimized.

Closed loop model tests

The main differences with computer simulations are:
- Environmental conditions are applied to maximum accuracy in laboratory conditions.

- Low frequency as well as high frequency effects are fully represented.
- Noise in the form of high frequency motion components are present in the position error, which makes it necessary to apply Kalman filtering before the positioning error can be inputted into the control system. An example of a control loop is given in Fig. 15.
- Accurate measurements can be made and the settings of the DP control system can be optimized in a realistic environment to achieve the most economic positioning.

Hence, the design information that is obtained from closed loop model tests is for final power selection of thrusters and optimized control coefficients. As an example the positioning of an export tanker during model tests in a 4 m sea state is shown for two concepts of tandem positioning in Fig. 16:
A. Fully stern positioning.
B. Stern following, but neglecting the surge motion of the storage tanker.

Fig. 17 shows that concept A requires about twice as much power consumption at the main propeller (in mean value and standard deviation) as concept B, while the positioning was similarly accurate in terms of separation distance between tankers.

FUTURE DEVELOPMENTS

So far a review of the state-of-the-art approaches for the design of moored and DP controlled tankers is given. The approaches concern both the semi-theoretical empirical mathematical models and physical model testing.

Further improvements in the semi-theoretical empirical mathematical models have to be carried out. Some of the developments are given below:
- wave drift-current interaction for arbitrary directions of waves and current and water depth;
- test duration for reliable statistical results;
- bow tunnel efficiency in waves;
- the application of adaptive control systems for optimum DP control routines;
- improvements of wave feed forward techniques;
- the hydrodynamic interaction between tandem moored tankers of which the initial work has been carried out as described in [10].

REFERENCES

1. Feikema, G.J. and Wichers, J.E.W.: "The effect of wind spectra on the low frequency motions of a moored tanker in survival condition", OTC paper No. 6605, 1991.
2. Pinkster, J.A.: "Low frequency second order wave exciting forces on floating structures", Doctor's thesis, University of Technology Delft, 1980.

3. Wichers, J.E.W.: "A simulation model for a single point moored tanker", Doctor's thesis, University of Technology Delft, 1988.
4. Wichers, J.E.W. and Huijsmans, R.H.M.: "Wave drift current interaction on a tanker in oblique waves", Proceedings of MARIN Workshop Hydrodynamics: Computations, Model Tests and Reality, MARIN, The Netherlands, May 1992.
5. Aalbers, A.B.: "Mooring and offloading: model testing for design", Third Offshore Symposium on FPSO Technology, SNAME Texas Section, Houston, February 1993.
6. Dercksen, A., Huijsmans, R.H.M. and Wichers, J.E.W.: "An improved method for calculating the contribution of hydrodynamic chain damping on low frequency vessel motions", OTC paper No. 6967, 1992.
7. Kat, J.O. de and Dercksen, A.: "The influence of spectral wave characteristics on the dynamics of a turret mooring system", OMAE'93, Edinburgh, 1993.
8. Aalbers, A.B. and Nienhuis, U.: "Dynamic positioning of tankers: Design aspects and recent developments", Symposium Floating Production Systems, London, 1989.
9. Nienhuis, U: "Analysis of thruster effectivity for dynamic positioning and low speed manoeuvring" Doctor's thesis, University of Technology Delft, 1992.
10. Feikema, G.J., Huijsmans, R.H.M. and Aalbers, A.B.: "Low frequency motions of tankers on tandem offloading condition", OTC paper No. 6945, 1992.

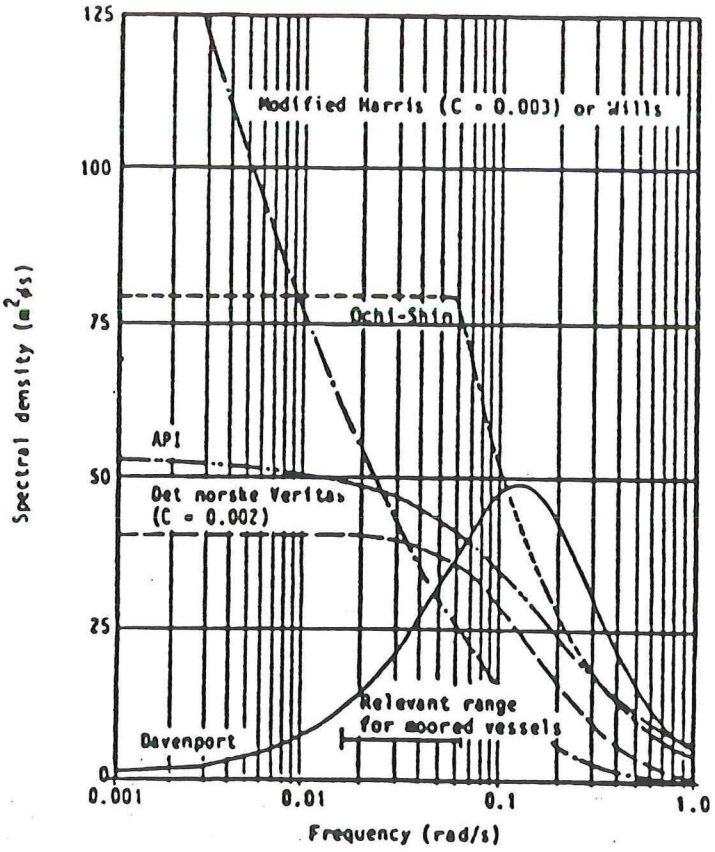

Fig. 1 - Spectral densities following the formulation of Harris-DnV, Davenport, Ochi-Shin, Wills and API wind spectra (V_W = 30.9 m/s; 10 m).

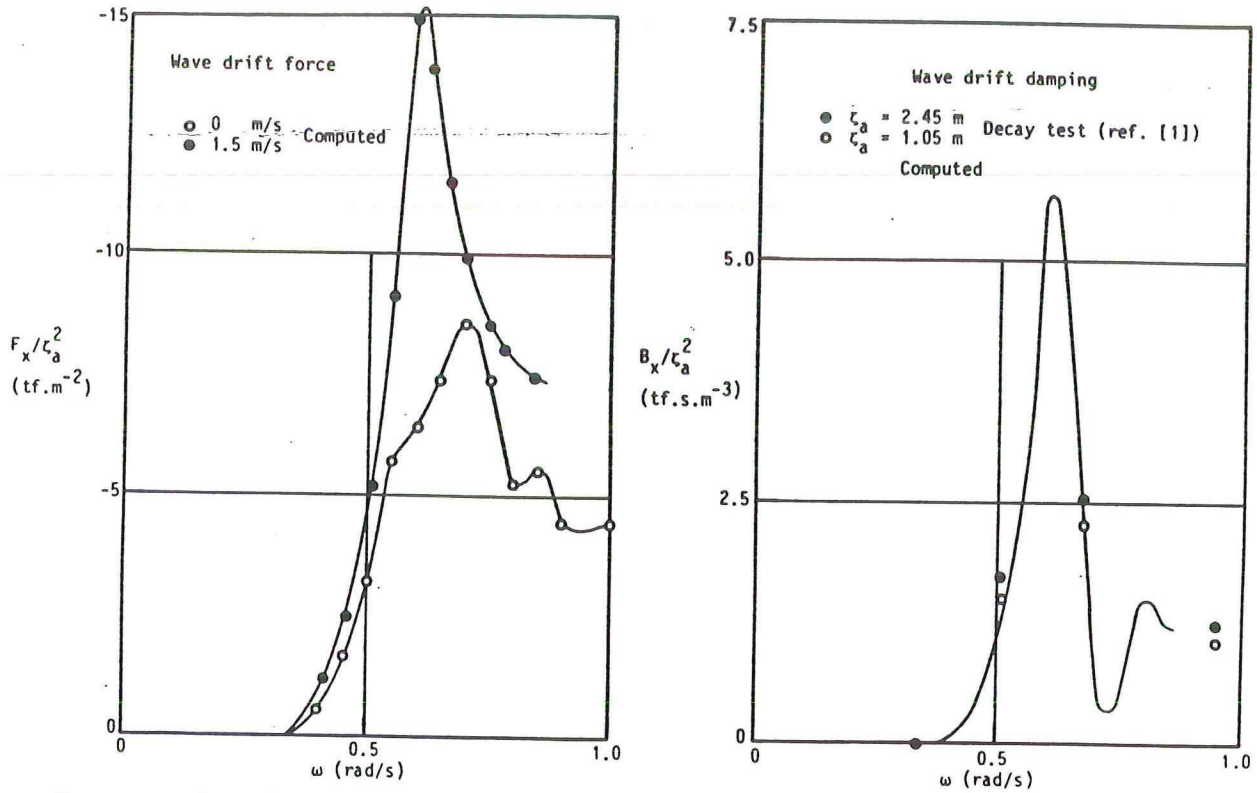

Fig. 2 - Quadratic transfer function of wave drift force and wave drift damping for an LNG tanker sailing in head waves (earth-bound wave frequencies).

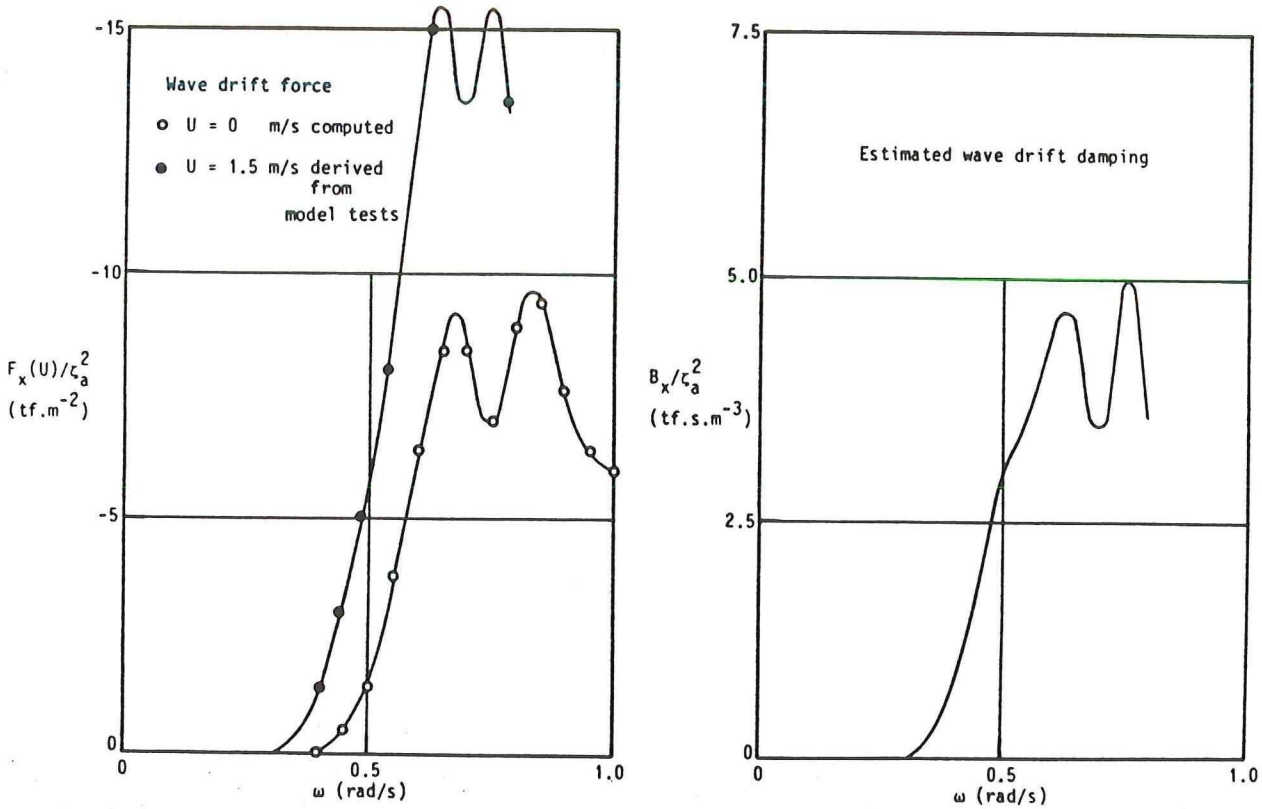

Fig. 3 - Quadratic transfer function of wave drift force and wave drift damping in bow quartering waves (earth-bound wave frequencies).

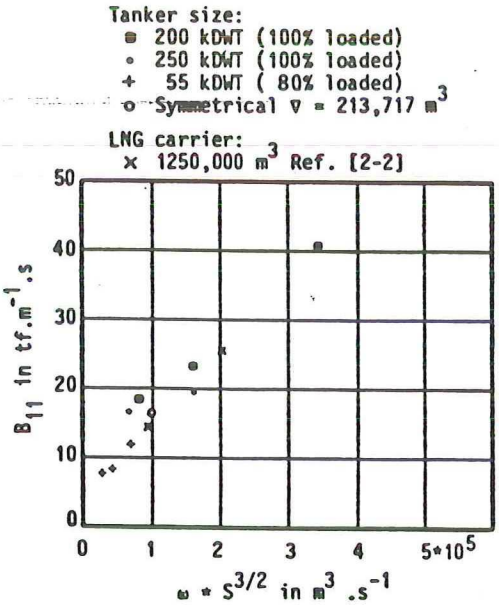

Fig. 4 - Measured viscous damping coefficient for the surge mode of motion as function of wetted hull area and surge frequency.

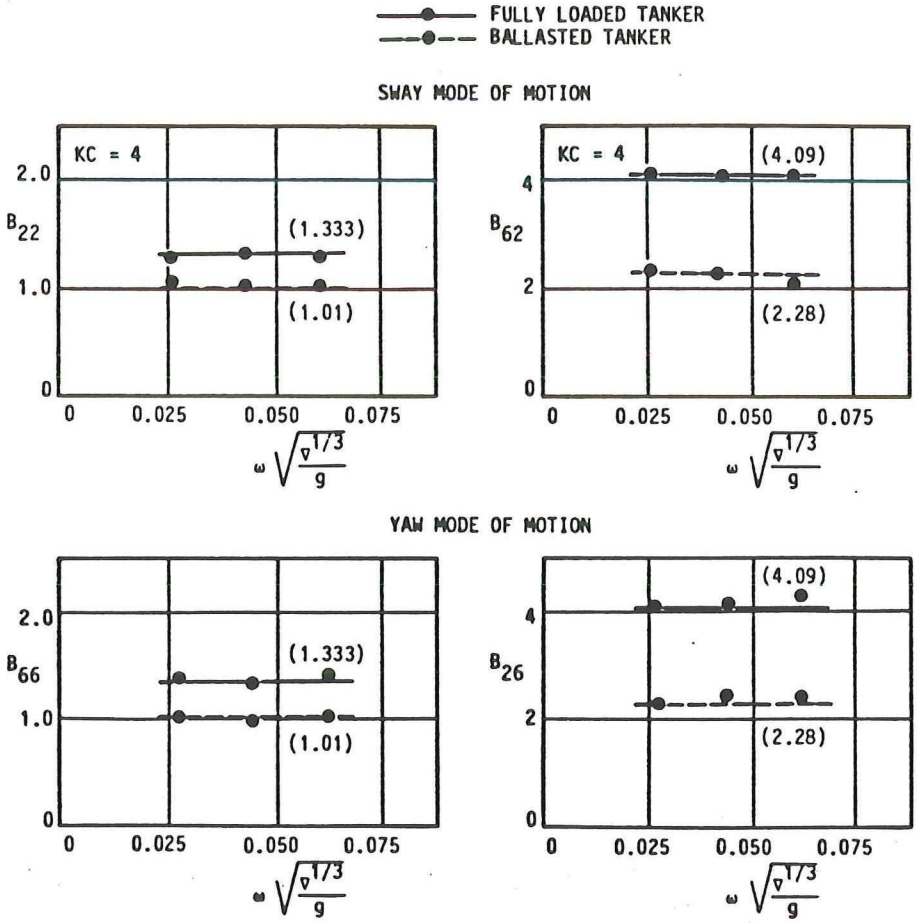

Fig. 5 - Low frequency viscous damping coefficients for the sway and yaw mode of motion in still water.

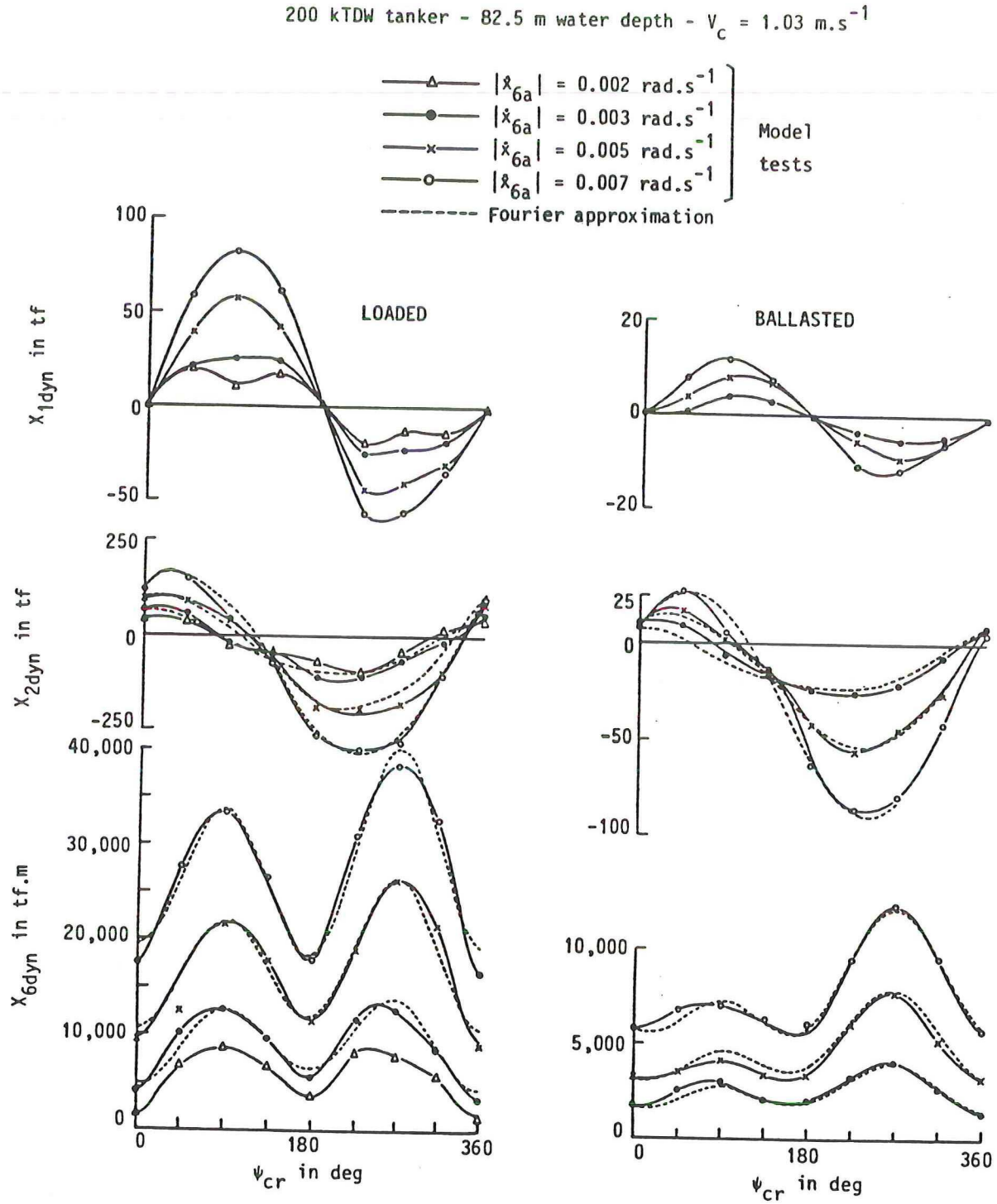

Fig. 6 - Dynamic current contributions in surge, sway and yaw direction due to motion in yaw direction in 2 knots current, based on negative yaw velocity.

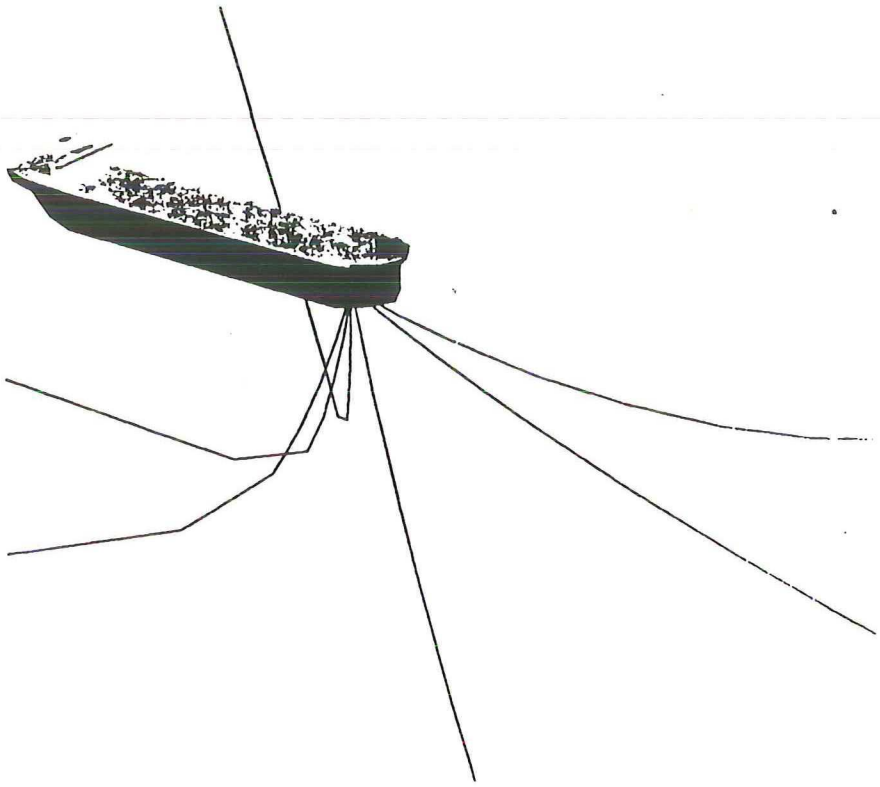

Fig. 7 - Turret moored tanker.

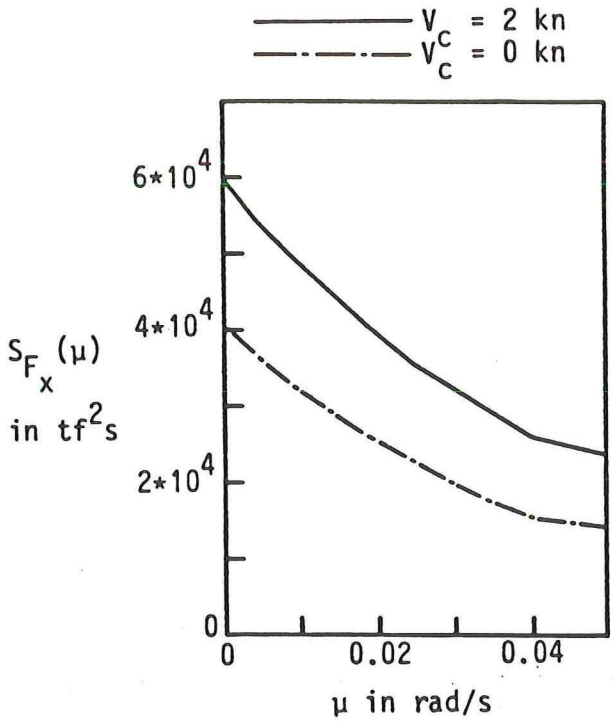

Fig. 8 - Computed spectral densities of the wave drift forces.

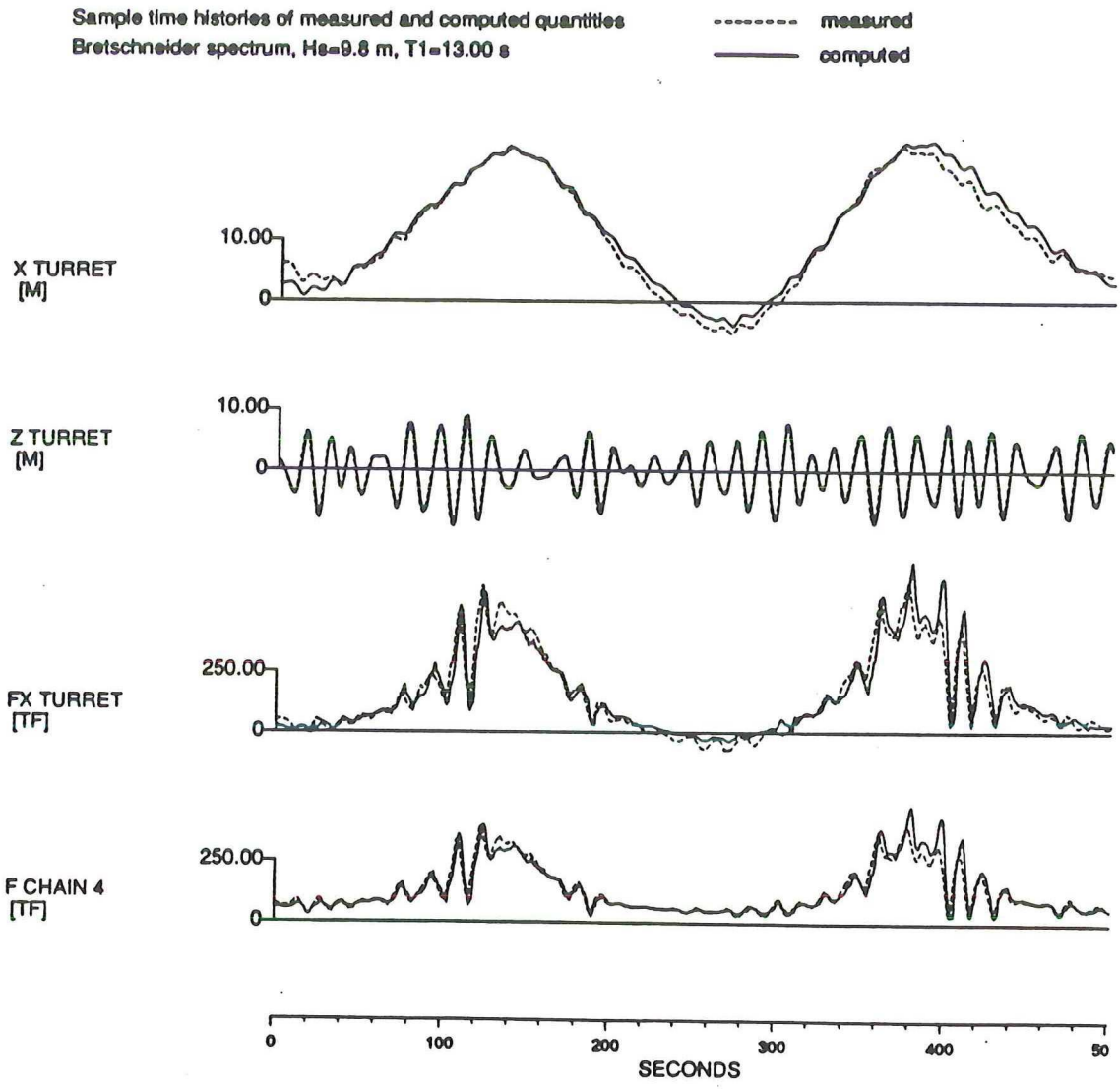

Fig. 9 - Sample time histories of measured and computed quantities.

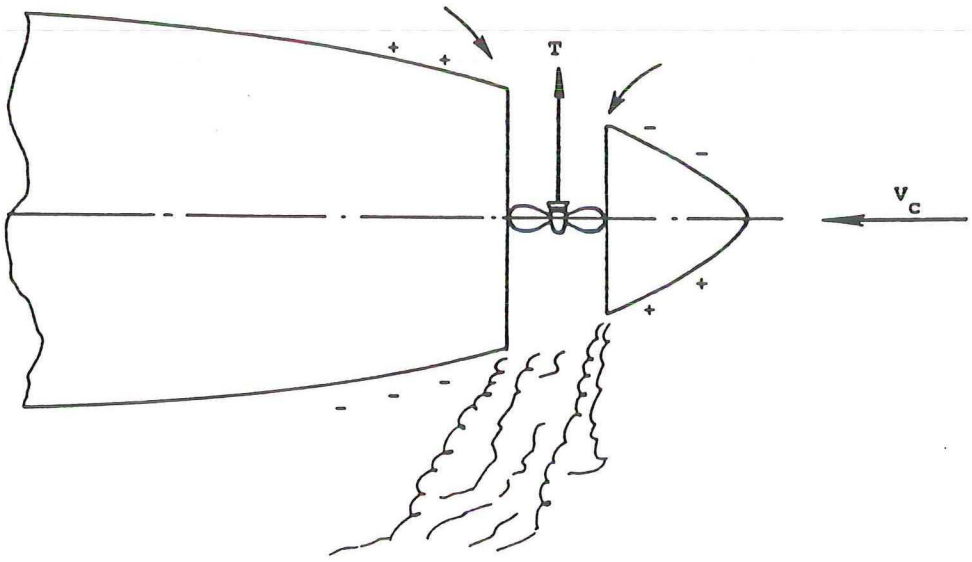

Fig. 10 - Bow thruster-current interaction.

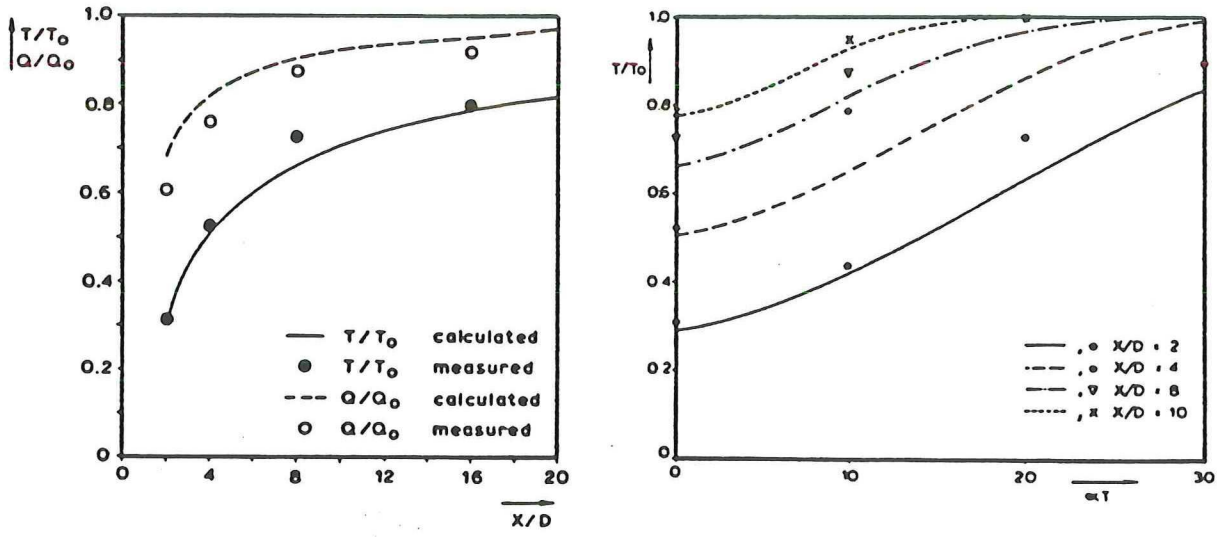

Fig. 11 - Thruster-thruster interaction under a flat plate as:
a) a function of distance between the two thrusters;
b) a function of azimuth angle of the forward thruster.

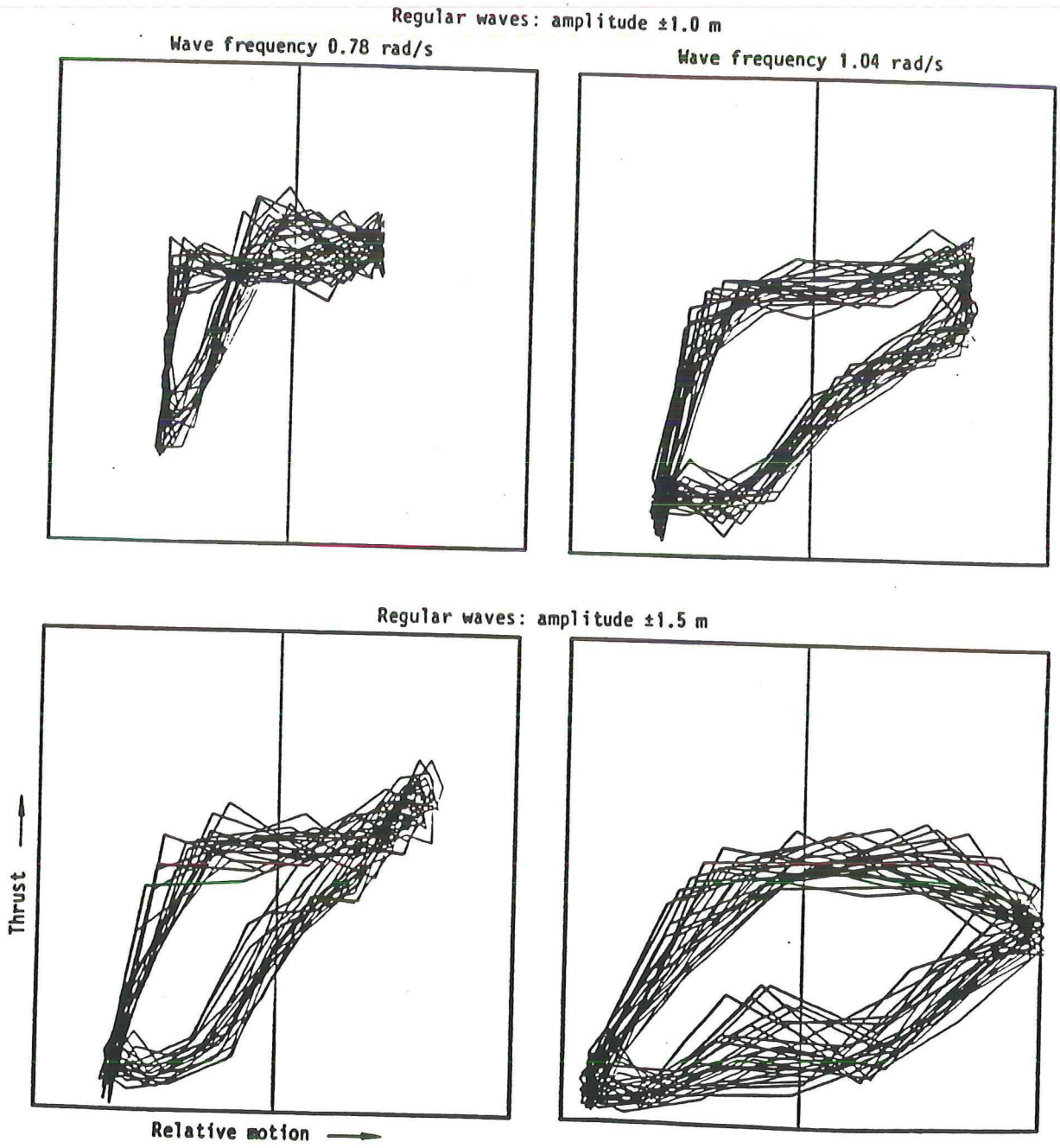

Fig. 12 - Thrust versus relative wave height at bow tunnel.

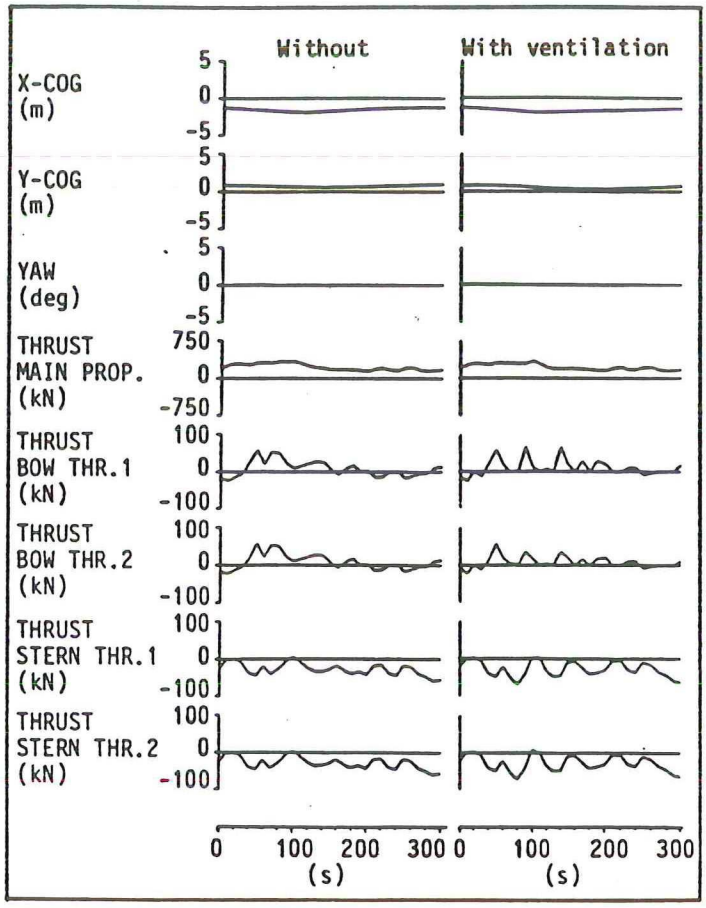

Fig. 13 - DP simulations showing the incident thrust loss after bow tunnel ventilation.

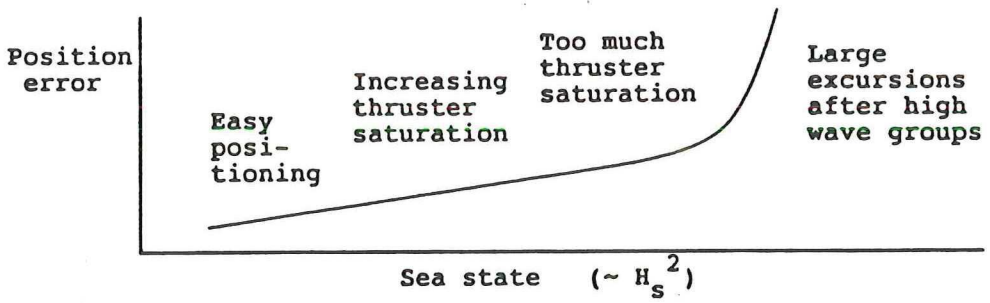

Fig. 14 - Limiting sea states for DP.

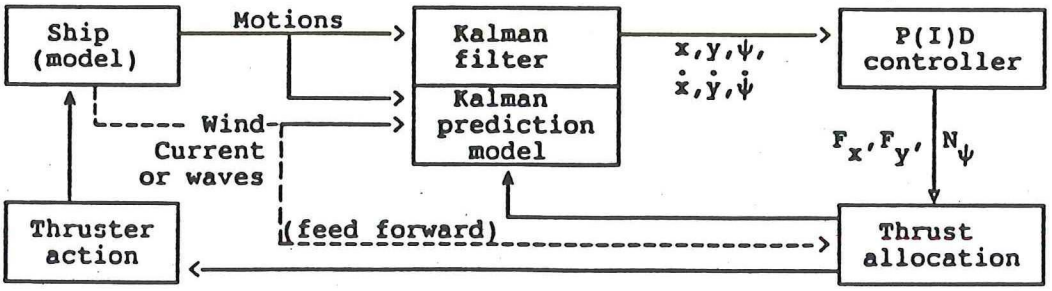

Fig. 15 - Example of control loop.

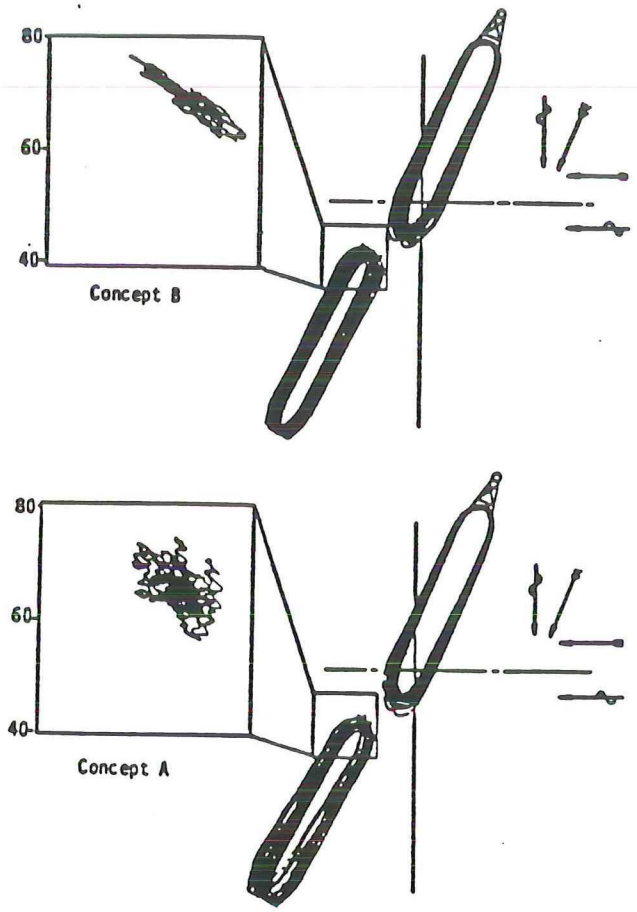

Fig. 16 - Tandem offloading for different DP concepts.

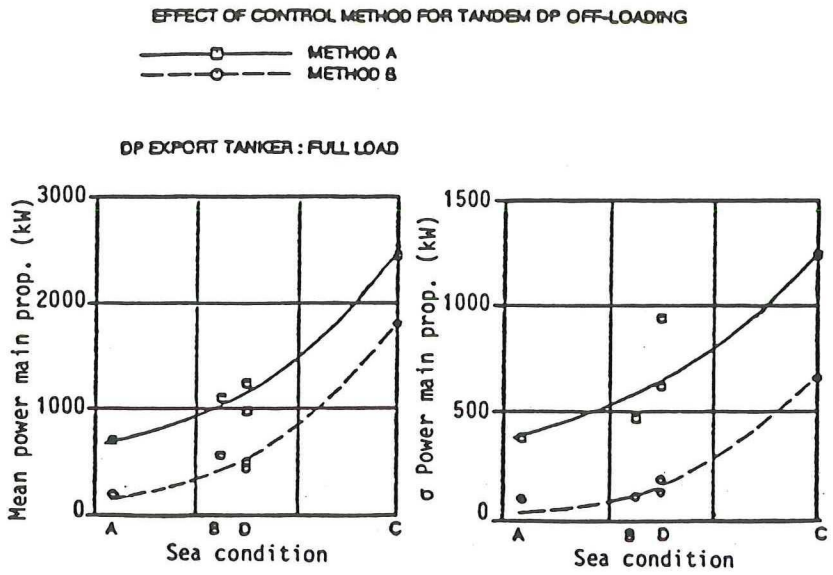

Fig. 17 - Main propeller power consumption.